

# Spin–Lattice Relaxation of the Tryptophan Triplet State Varies with Its Protein Environment

Andrzej Ozarowski, Ajay Misra, Sanjib Ghosh,<sup>†</sup> and August H. Maki\*

Department of Chemistry, University of California, Davis, Davis, California 95616

Received: November 20, 2001; In Final Form: February 20, 2002

Spin–lattice relaxation (SLR) has been studied at 1.2 K in the photoexcited triplet state of tryptophan (Trp) in a number of protein sites in zero applied magnetic field. We find that there is a distribution of SLR rate constants in every case that indicates the partitioning into two populations,  $n_s^0$  and  $n_t^0$ , with differing behavior.  $n_s^0$  undergoes slow SLR with rate constants in the range found in crystalline matrixes, while the SLR of  $n_t^0$  is at least 1–2 orders of magnitude faster. The former population has considerable spin alignment during optical pumping, decays nonexponentially, and gives rise to optically detected magnetic resonance (ODMR) responses at 1.2 K. The latter has negligible spin alignment, decays largely as a single exponential, and is ODMR silent. The rapid SLR of  $n_t^0$  is attributed to coupling with disorder (tunneling) modes that modulate the electron–electron dipolar coupling, and whose efficiency varies with protein site. The less efficient SLR of  $n_s^0$  is the result of direct interaction with lattice phonons. We find no correlation of the distribution of populations with the heterogeneity of the protein site as determined by ODMR bandwidth. It is suggested that more efficient disorder mode-induced SLR is associated with decreased rigidity of the local environment.

## Introduction

The study of electron spin–lattice relaxation (SLR) of paramagnetic impurities in solids has emerged as a useful approach that yields information about the structure of the matrix, and the nature of guest–host interactions.<sup>1</sup> Much of the early work on SLR was carried out on transition metal ions<sup>2</sup> and free radicals<sup>3,4</sup> in crystalline solids. SLR measurements of the photoexcited triplet states of aromatic molecules in crystals were first reported by Wolfe,<sup>5</sup> and subsequently by other investigators.<sup>6–10</sup>

Although the interpretation of SLR in crystals follows from ideas elaborated by van Vleck,<sup>2,11</sup> the process differs significantly in disordered solids. SLR of free radicals in a frozen glass matrix at cryogenic temperature is orders of magnitude more efficient than it is in a crystalline matrix;<sup>12</sup> this also is the case for photoexcited triplet states of aromatic molecules.<sup>13–16</sup> In low temperature glasses, SLR follows an approximately  $T^2$  dependence rather than  $T^1$  (direct phonon process) and  $T^5$  or  $T^7$  (phonon scattering process) found in crystalline samples.<sup>1,2</sup> SLR in glasses is believed to be dominated by coupling of the spins to disorder (tunneling) modes that modulate the electron–(solvent) nuclear dipole (END) interaction in the case of free radicals<sup>12</sup> or the electron–electron dipolar (EED) coupling in the case of triplet states.<sup>14–16</sup> These disorder (tunneling) modes have been modeled as two-level systems,<sup>17,18</sup> and can account for the low-temperature specific heat and other anomalous properties of glasses.<sup>19</sup>

In previous work,<sup>10,20</sup> we have used optically detected magnetic resonance in zero applied magnetic field (ODMR)<sup>21</sup> to investigate SLR in the photoexcited triplet state of tryptophan (Trp) in aqueous ethylene glycol (EG) glass at cryogenic temperature (ca. 1.2 K). In zero applied magnetic field, ODMR

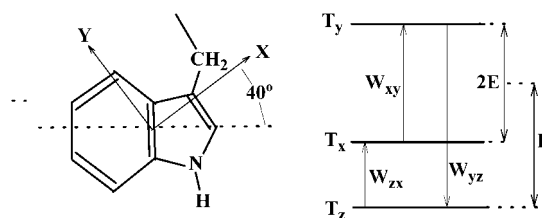


**Figure 1.** Energy level diagram of the triplet state of Trp in zero applied magnetic field. The ZFS parameters,  $D$  and  $E$  are indicated. The principal axes corresponding to the ZF sublevels  $T_x$ ,  $T_y$ , and  $T_z$  of Trp are shown at the left. Three SLR transitions are shown as vertical arrows on the energy level diagram. For Trp,  $D = 3.01$  GHz, and  $E = 1.24$  GHz.

bands occur at frequencies given by  $D - E$  ( $T_z \leftrightarrow T_x$ ),  $2E$  ( $T_x \leftrightarrow T_y$ ), and  $D + E$  ( $T_y \leftrightarrow T_z$ ), where  $D$  and  $E$  are the zero field splitting (ZFS) parameters<sup>22</sup> of the triplet state. Figure 1 shows the ZFS pattern of tryptophan.

Kinetic information of the triplet state is obtained frequently using the microwave-induced delayed phosphorescence (MIDP) experiment<sup>23</sup> in which the phosphorescence is monitored during its decay while a microwave pulse or rapid passage is applied to an ODMR transition following a variable delay. Kinetic information is obtained from the shape of the phosphorescence transient, and from a semilogarithmic plot of its peak intensity vs delay.<sup>23</sup> Conventional MIDP analysis yields accurate sublevel decay constants only if SLR is negligible; otherwise, the method yields only apparent values that are mixed with SLR kinetics. Even at the lowest temperatures used in MIDP measurements, ca. 1.2 K, the SLR rate constants of Trp are not negligible because of its small sublevel decay constants.<sup>21</sup> It is now possible, however, using global analysis of digitally collected MIDP data sets<sup>24</sup> that contain upward of 15 000 data points to obtain accurate values of the individual sublevel decay constants,  $k_i$ , the SLR rate constants,  $W_{ij}$ , the relative radiative rate constants,  $r_{ix}$  ( $=k_{ix}/k_x$ ), and the relative initial sublevel populations. In the preceding,  $i, j = x, y, z$  label the triplet sublevels,

\* To whom correspondence should be addressed. Phone: (530) 752-6471. Fax: (530) 752-8995. E-mail: maki@indigo.ucdavis.edu.

<sup>†</sup> Permanent address: Department of Chemistry, Presidency College, Calcutta 700073, India.

where  $x$ ,  $y$ , and  $z$  are the principal axes of the tryptophan ZFS tensor<sup>22</sup> whose directions are shown in Figure 1 as are the relative energies of the sublevels.  $T_x$  is the shortest-lived and most radiative, while  $T_z$  is the longest-lived and least radiative sublevel.<sup>21</sup> Using global analysis of MIDP data sets, we have found,<sup>24</sup> for example, that within experimental error,  $k_z = r_{zx} = 0$  for Trp. The initial step in the major decay routes of  $T_z$  to the ground state is SLR to either  $T_x$  or  $T_y$ .

Since the kinetic and radiative parameters of the triplet state as well as the initial relative sublevel populations can be obtained from the MIDP data using global analysis,<sup>24</sup> all the information is available to predict the phosphorescence decay at the temperature of the MIDP measurements. We have attempted to fit the phosphorescence decay of Trp and of the single Trp residue of ribonuclease T1 from *Aspergillus oryzae* (RNase T1) in aqueous EG low-temperature glasses to the parameters obtained from global MIDP analysis.<sup>20</sup> We found that the triplet state population does not follow the predicted decay; the semilogarithmic plot of the decay has in each case less curvature than is predicted. The results could be interpreted, however, in terms of a *distribution* of the SLR rate constants. Moreover, it was found that for Trp and RNase T1, the distribution of SLR appears bimodal, with an initial population,  $n_s^0$ , that undergoes slow SLR and is responsible for the MIDP responses, and a second initial population,  $n_f^0$ , that undergoes fast SLR and is effectively MIDP silent. Aside from a minor initial rapid transient,  $n_f^0$  decays as a single exponential with rate constant,  $k_1 \approx k_{av} = (\sum k_i)/3$ , which is the expected behavior since the  $W_{ij}$  exceed the  $k_i$  for this population.<sup>8</sup> The phosphorescence of  $n_s^0$ , on the other hand, decays nonexponentially and as predicted by the kinetic and radiative parameters obtained from global MIDP analysis. Although there is probably a considerable distribution of slr rate constants in the rapidly relaxing population,  $n_f^0$ , deconvolution of the phosphorescence kinetics as a bimodal distribution is possible for Trp since a negligible number has  $W_{ij} \approx k_i$ .

Subsequent study<sup>10</sup> in which triplet states in crystalline matrixes were compared with those in disordered glassy matrixes demonstrated that the crystalline samples did not exhibit a rapidly relaxing population, and thus the  $n_f^0$  population is associated with the glassy matrix. In addition, the size of the  $W_{ij}$  found for triplet states in crystalline samples is the same as those found for  $n_s^0$  in glass samples, and more than an order of magnitude smaller than those estimated<sup>10</sup> for  $n_f^0$ . Thus, we concluded that (a) the slow SLR rates are due to direct absorption and emission of lattice phonons in both crystalline and disordered samples<sup>2,25</sup> (the Raman process should be negligible at 1.2 K, the temperature of the MIDP measurements), and (b) the rapid slr results from the existence of disorder (or tunneling) modes<sup>19</sup> in disordered solids, and the coupling of these modes to a sub-population of the triplet states whose spins are relaxed thereby due to modulation of the EED interaction.<sup>14–16</sup>

We report in this work on the variation of the SLR of the tryptophan triplet state with its location in a number of proteins whose ODMR we have studied previously at 1.2 K. The distribution of SLR should provide information about the degree of disorder mode activity within protein sites, and their coupling to the indole chromophore of tryptophan. To the extent that the local environment of tryptophan exhibits the ordered and rigid character of a genuine crystal, the rapid SLR associated with  $n_f^0$  should be absent. Thus the fraction of rapidly relaxing triplet states,  $\Phi_f = n_f^0/(n_f^0 + n_s^0)$ , may be useful in characterizing the crystalline nature of tryptophan sites in proteins, and the activity of disorder modes. In previous work on tryptophan and the

single tryptophan residue of RNase T1,<sup>10</sup> it was found that  $\Phi_f$  varies with the composition of the EG–water (or aqueous buffer) glass and has a broad minimum in the 30–40% EG by volume (v/v) range. In the following, we find that  $\Phi_f$  varies considerably among protein sites, but does not correlate with the local heterogeneity as determined by the ODMR bandwidth. The minimum value of  $\Phi_f$  among the proteins investigated occurs in *Escherichia coli* alkaline phosphatase (AP) which also exhibits an unusually long room-temperature phosphorescence (RTP) lifetime.<sup>26</sup> In the absence of quenching, RTP lifetime increases with local viscosity and thus with the rigidity of the protein environment.<sup>27</sup> We suggest, therefore, that disorder mode activity in proteins at low temperature may have an inverse relationship to RTP lifetime.

## Experimental Section

**Materials.** Sources of Trp and RNase T1 are given previously.<sup>20</sup> These samples are studied in water or pH 7 phosphate buffer with EG added as cryosolvent to 40 vol %. Trp concentration is 1 mM, while that of RNase T1 is 0.2 mM. The effect of dissolved O<sub>2</sub> on SLR of Trp is assessed by comparison of Ar purged, air equilibrated and O<sub>2</sub> saturated samples. Effects of solvent deuteration are assessed, as well. For these measurements, Trp is dissolved in 40% v/v EG-*d*<sub>6</sub> (99% D, Acros Organics)–D<sub>2</sub>O (99.5% D).

Single tryptophan-containing mutants of lactose repressor protein from *E. coli* (LacRep) are a generous gift from Prof. Kathleen Matthews of Rice University. Construction of these mutants<sup>28,29</sup> and their investigation by fluorescence<sup>30</sup> and ODMR<sup>29</sup> has been described previously. Samples are dialyzed into 0.1 mM potassium phosphate buffer, pH 7.4, containing 30% (v/v) EG. Complexes with the inducer, isopropyl  $\beta$ -D-thiogalactoside (IPTG) are prepared by adding concentrated IPTG at a molar ratio of 200:1, as described previously.<sup>29</sup> Concentrations are ca. 1 mM in monomer.

Doubly mutated tryptophan-free tryptophan repressor from *E. coli* (W19, 99/F trpRep) was generously supplied by Prof. Maurice Eftink, University of Mississippi. Its synthesis using site-directed mutagenesis has been described.<sup>31</sup> Details of the preparation of the holorepressor complex from apo trpRep and its study by ODMR have been given earlier.<sup>32</sup> The mutated apo trpRep is dissolved in 10 mM, pH 7, phosphate buffer, and incubated with equimolar Trp corepressor to form the holorepressor complex. EG is added to 40% (v/v). The final concentration of holorepressor is  $5 \times 10^{-4}$  M.

Alkaline phosphatase from *E. coli* (AP) was purchased from Sigma (Type III, chromatographically purified suspension in 2.5 M (NH<sub>4</sub>)<sub>2</sub>SO<sub>4</sub>, activity: 43.7 u/mg protein). AP is exchanged into 100 mM Tris buffer, pH 8, containing 1 mM Na<sub>2</sub>HPO<sub>4</sub>, 0.1 mM MgCl<sub>2</sub>, and 0.1 mM ZnCl<sub>2</sub>. A sample of mutated AP (W220Y AP) was kindly donated by Prof. Ari Gafni, University of Michigan. Its construction has been described earlier.<sup>33</sup> W220Y AP is studied in 10 mM EPPS buffer, pH 7.5 containing 100 mM NaCl, 1 mM Na<sub>2</sub>HPO<sub>4</sub>, 1 mM MgCl<sub>2</sub>, and 1 mM ZnCl<sub>2</sub>. EG is added to 30% (v/v). The final concentration of W220Y AP is  $3 \times 10^{-5}$  M. ODMR measurements on AP have been completed recently.<sup>34</sup>

The source of NCp7, the nucleocapsid protein of human immunodeficiency virus type 1 is given earlier.<sup>35</sup> It is studied at ca. 0.3 mM concentration in a 10 mM sodium phosphate pH 7.2 glass containing 30% EG by volume. The complex with polyinosinic acid (poly I) is studied, as well, at a 5:1 ribophosphate to NCp7 molar ratio.

The water used is deionized and distilled in a quartz still. All reagents and solvents are of the purest quality available.

**Methods.** Samples, 30–50  $\mu\text{L}$ , are contained in a 2 mm inside diameter Suprasil quartz tube inserted into a copper helix that terminates a coaxial stainless steel microwave transmission line. This structure is inserted into a stainless steel dewar with quartz optical windows in which the sample can be held at 77 K (boiling  $\text{N}_2$  temperature), 4.2 K (immersed in boiling He) or 1.2 K (immersed in vacuum-pumped He) for low temperature phosphorescence and ODMR measurements that are made in zero applied magnetic field. Details of the phosphorescence and ODMR spectrometer that uses photon counting have been described previously.<sup>24,36</sup> Digital signal averaging is employed for all ODMR and phosphorescence decay measurements. Center frequencies,  $\nu_0$ , and bandwidths,  $\nu_{1/2}$  of the ODMR bands are obtained using algorithms described earlier for steady state,<sup>36</sup> and delayed<sup>37</sup> slow passage ODMR. Kinetic rate constants, radiative parameters, and relative sublevel populations are obtained from global analysis of MIDP measurements as described earlier.<sup>24</sup>

The phosphorescence decay is collected through a monochromator set at the maximum of the Trp phosphorescence 0,0-band using 3 nm bandwidth. At 4.2 K, SLR of the entire Trp population is rapid,<sup>21</sup> and the kinetics are fit to a single exponential using a nonlinear least squares procedure. This is taken as the mean low temperature decay constant of the Trp triplet state. In the event that there is a measurable tyrosine component that underlies the Trp 0,0-band, the pure tyrosine decay at 4.2 K is recorded at a wavelength to the blue of the Trp 0,0-band. This decay is weighted by its contribution to the steady state intensity and digitally subtracted from the decay recorded at the Trp 0,0-band wavelength to yield the Trp contribution that is then fitted to a single-exponential decay with lifetime,  $\tau_{\text{av}}$ , as described above.

At 1.2 K, a portion of the Trp population,  $n_s^0$ , is characterized by slow SLR, as discussed above, and decays nonexponentially, while the remainder  $n_f^0$ , decays exponentially with lifetime  $\tau_1$  (aside from a minor initial transient). For Trp,  $\tau_1 \geq \tau_{\text{av}}$ ; this will be discussed in the following section. The kinetic and radiative parameters of  $n_s^0$  obtained from global analysis of MIDP are used to calculate its predicted nonexponential decay. This calculated decay is weighted in such a manner, using trial and error, that when subtracted from the recorded Trp decay at 1.2 K the remainder is a single exponential. The resulting initial intensities of  $n_s^0$  and  $n_f^0$ , namely  $I_s^0$  and  $I_f^0$  respectively, are not proportional to the populations, since  $n_s^0$  has considerable spin alignment whereas  $n_f^0$  has none (aside from the minor spin alignment during optical pumping responsible for an initial transient in the decay). The populations and intensities are related by<sup>20</sup>

$$n_s^0/n_f^0 = [(\sum r_{ix})(\sum n_{ix}^0)/3(\sum r_{ix}n_{ix}^0)][I_s^0/I_f^0] \quad (1)$$

where  $i = x, y, z$ , and  $n_{ix}^0$  are the initial relative sublevel populations,  $n_i^0/n_x^0$ , obtained from global MIDP analysis.  $I_f^0$  is the initial intensity of the single-exponential decay component *minus the initial transient*. The decay constant that characterizes the major component of the decay of  $n_f^0$  at 1.2 K is the smallest eigenvalue of the rate constant matrix,  $k_1$ . The initial minor transient of this population consists of the two larger eigenvalues,  $k_2$  and  $k_3$ . We find that the residuals of the fitting are very sensitive to the  $I_s^0$  and  $I_f^0$  obtained by the trial and error weighting of the slow slr component, and that they are generally reliable to 1–2%.

In a few cases, underlying tyrosine phosphorescence complicates the analysis of the Trp decay at 1.2 K. In this case, the tyrosine decay is recorded at 1.2 K to the blue of the Trp

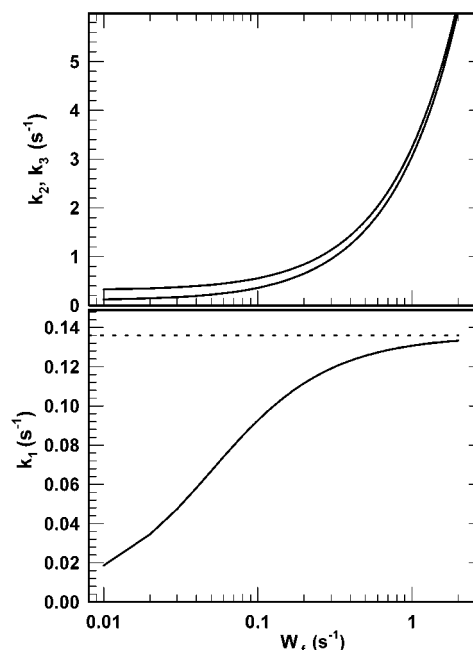


**Figure 2.** Calculated eigenvalues of the Trp triplet state are plotted vs the SLR rate constant  $W_f$ , which is assumed to be isotropic; see text. The assumed  $k_i$  ( $i = x, y, z$ ) are those of Trp, given in Table 1.  $k_1$  becomes the major amplitude component of the nonexponential decay when  $W_f$  becomes large, while the amplitudes represented by the larger rate constants,  $k_{2(3)}$  tend toward zero under this condition. The dashed line represents  $k_{\text{av}}$  of Trp, which is the limit approached by  $k_1$  as  $W_f$  increases.

emission as described above, weighted by its contribution to the emission recorded at the Trp 0,0-band peak, and subtracted to yield the Trp component. The latter is then fitted to contributions from  $I_s^0$  and  $I_f^0$  as outlined above. The uncertainty of the result is somewhat larger in this case because of additional error introduced in removing the tyrosine contribution.

**Relaxation Model for the Population with Rapid SLR.** The phosphorescence decay of the population  $n_f^0$  is the sum of an exponential with decay constant  $k_1$ , and a minor initial bi-exponential transient with decay constants  $k_2$  and  $k_3$ . These are the eigenvalues of the rate constant matrix, and *in the limit where the  $k_i$  can be neglected with respect to much larger SLR rate constants*, they are<sup>8</sup>

$$k_1 = 1/3(k_x + k_y + k_z) = k_{\text{av}} \quad (2)$$

$$k_{2(3)} = W_{xz} + W_{yz} + W_{xy} \pm [W_{xz}(W_{xz} - W_{yz}) + W_{yz}(W_{yz} - W_{xy}) + W_{xy}(W_{xy} - W_{xz})] \quad (3)$$

We do not have information about the anisotropy of SLR in the  $n_f^0$  population, nor about its distribution. To obtain some information about the magnitude of SLR in this population, we adopt a simplified isotropic model where each  $W_{ij} = W_f$ , and that the  $k_i$  are the same as they are for  $n_s^0$ . Using the  $k_i$  for Trp<sup>24</sup>, we have calculated  $k_1$ ,  $k_2$ , and  $k_3$  for a range of  $W_f$ . These are shown plotted in Figure 2 over the range  $0.01 \text{ s}^{-1} \leq W_f \leq 2 \text{ s}^{-1}$ . Note that  $k_1$  is less than  $k_{\text{av}}$  but approaches it over this range of  $W_f$ , while  $k_2$  and  $k_3$  approach  $3W_f$  with increasing  $W_f$  as expected from eq 3 which is valid for  $W_f \gg k_i$ .

## Results

In Figure 3 is shown the treatment of a data set, that of H74W LacRep at 1.2 K, according to the procedure outlined in the previous section. The sample is a mutated protein (described



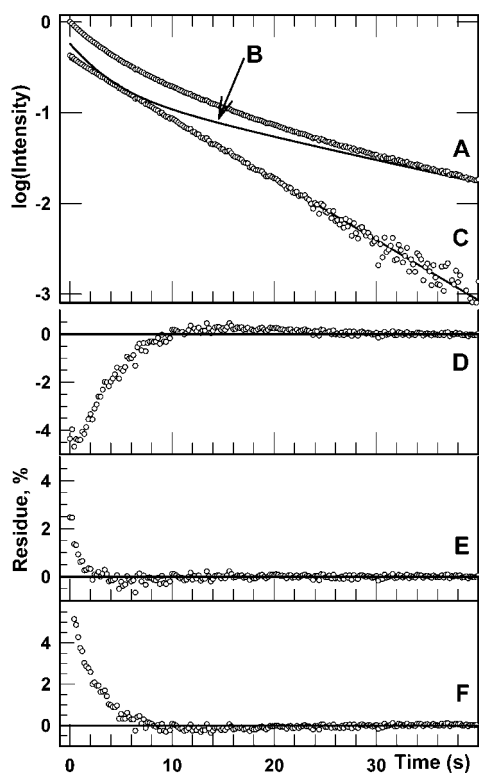


**Figure 3.** Analysis of the phosphorescence decay of H74W LacRep (Trp<sup>74</sup>) at 1.2 K monitored at its 0,0-band maximum (Table 1) with 3.2 nm bandwidth. The experimental decay is shown in (A). (B) is the predicted decay of the population  $n_s^0$  scaled to 0.575 of the initial intensity. (C) is curve (B) subtracted from (A) and fitted with the single exponential  $0.400 \exp(-0.155t)$ , the result of least-squares minimization. (D) is a residuals plot of the experimental curve from which is subtracted the predicted decay of  $n_s^0$  scaled to 0.595 of the initial intensity, (E) is the residuals plot of (C), and (F) is a residuals plot with scaling of the predicted decay of  $n_s^0$  to 0.555 of the initial intensity. From the best fit, (C),  $k_1 = 0.155 \text{ s}^{-1}$ ; the initial transient ( $\sim 2.5\%$  of the initial intensity) that is visible in (E) is the short-lived component of the decay (see text). Only every fifth data point is plotted in each experimental plot.

below) in which the single Trp has been substituted for histidine at position 74.<sup>28–31</sup> Residuals are shown for the best-fit decay of  $n_i^0$ ,  $0.400 \exp(-k_1t)$ , as well as poorer fits for which the preexponential factor is changed to 0.380 and 0.420. Comparison of residuals demonstrates that for H74W LacRep and for the other samples without interfering Tyr emission, the intensity of the  $n_i^0$  population is accurate to far better than  $\pm 0.02$ . The best-fit residuals plot of Figure 3 also reveals a minor transient that could be attributed to the component of  $n_i^0$  with decay constants  $k_{2(3)}$ .

Values of  $k_1$  and  $\Phi_f$  for Trp in various situations are given in Table 1. Also included are kinetic parameters of the sublevels and ODMR bandwidths of the  $D - E$  and  $2E$  ODMR transitions from previous work.

## Discussion

### Dissolved Oxygen and Deuteration Effects on Tryptophan.

Dissolved oxygen severely reduces the lifetime of triplet states in low viscosity liquids, and its removal is necessary for the observation of RTP.<sup>26</sup> Oxygen is not considered a problem in low-temperature glasses, however, and it is not removed for ODMR measurements, in general. Comparison of the data for Trp in air-equilibrated and Ar-purged EG–water (Table 1) reveals no significant differences in kinetic properties, suggesting that  $\text{O}_2$  removal normally is not necessary for ODMR studies

at low temperature. When saturated with  $\text{O}_2$ , however, changes in SLR behavior are found.  $\Phi_f$  increases from 0.38 (Ar) to 0.48, indicating that dissolved  $\text{O}_2$  at this concentration enhances the efficiency of disorder mode relaxation. The kinetic constants of  $n_s^0$  are not affected greatly, except for an enhancement of  $W_{xy}$ , the smallest SLR parameter in free Trp. Dissolved  $\text{O}_2$  molecules in the vicinity of a Trp triplet state could induce SLR through fluctuating magnetic fields produced if coupled to the disorder mode structure of the glass. This mechanism is analogous to the END mechanism proposed for free radical SLR in low-temperature glasses,<sup>12</sup> except that the relaxing agencies are now paramagnetic  $\text{O}_2$  molecules, rather than nuclear spins.

Noticeable changes occur in the deuterated solvent, although there is no significant change in  $\Phi_f$  (Table 1). The decay constant,  $k_{av}$ , is reduced by ca. 9%, and the apparent heterogeneity of the environment, as indicated by the  $\nu_{1/2}$ , increases. The longer lifetime may result largely from deuteration of the ring N–H proton of Trp, reducing out-of-plane vibrations that are important in inducing intersystem crossing, as suggested by Fischer et al.<sup>33</sup> to explain the effect of protein deuteration on the RTP kinetics of AP. Deuteration of an aromatic molecule at a single site reduces the radiationless decay rate constants slightly at low temperature. Monodeuteration of benzene leads to a ca. 6% reduction in phosphorescence rate constant at 77 K,<sup>38</sup> and monodeuteration of naphthalene has a similar effect.<sup>39</sup> The effect of ring monodeuteration may be larger at elevated temperatures.<sup>33</sup> Deuteration of the glass matrix should have little effect on the decay rate constants except possibly at elevated temperature.<sup>40</sup>

**Alkaline Phosphatase.** In recent ODMR studies of AP,<sup>34</sup> we characterized the three Trp residues at positions 109, 220, and 268. Data for Trp<sup>109</sup> and Trp<sup>220</sup>, that have cleanly resolved 0,0-band origins at 414.5 and 411.4 nm, respectively, are given in Table 1. Trp<sup>109</sup> is a buried residue in the hydrophobic core that is considered to be responsible for the unusually long-lived RTP.<sup>26,41</sup> Its phosphorescence spectrum has among the narrowest bandwidths of Trp sites in proteins, and its ODMR bandwidths are three times narrower than any previously observed. The environment of Trp<sup>109</sup> is unusually homogeneous. Trp<sup>220</sup> has a far less homogeneous environment based on phosphorescence and ODMR bandwidth criteria, and is more nearly typical of protein sites.<sup>21</sup> If Trp<sup>109</sup> were located in a “crystalline environment”, we would expect the absence of disorder modes and  $\Phi_f = 0$ . Instead, we find  $\Phi_f = 0.30$  for Trp<sup>109</sup> in wild type (wt) AP and 0.33 in W220Y AP, indicating disorder mode activity, but at a lower level than for free Trp in EG–water (0.35 in air saturated, 0.38 in argon purged solvent). On the other hand,  $\Phi_f = 0.30$  for Trp<sup>220</sup> in wt AP, as well, although Trp<sup>220</sup> resides in a far less homogeneous environment than Trp<sup>109</sup>. This result, and other results to be discussed below, demonstrate that disorder mode activity does not correlate with site heterogeneity.

**Lactose Repressor Protein.** Three single tryptophan-containing LacRep proteins and their complexes with IPTG were analyzed and these data are presented in Table 1. Two of these, H74W LacRep and Y273W LacRep are triple mutants, based on a Trp-free construct in which the native Trp<sup>201</sup> and Trp<sup>220</sup> have been substituted with tyrosine, and a single Trp is introduced at positions 74 and 273, respectively.<sup>28,31</sup> The third, W201Y LacRep, has Trp<sup>201</sup> substituted with tyrosine leaving a single Trp at position 220. The effects of structural changes induced by IPTG binding on the triplet state properties of these LacRep mutant proteins have been reported earlier.<sup>29</sup> The Trp residues in the LacRep mutants studied are located in the core domain of the tetrameric protein, and ligand binding produces

TABLE 1: Kinetic Parameters and ODMR Bandwidths of Tryptophan<sup>a</sup>

sample/ $\lambda_{0,0}$ <sup>b</sup>	$k_x$ (s <sup>-1</sup> )	$k_y$ (s <sup>-1</sup> )	$k_z$ (s <sup>-1</sup> )	$W_{xy}$ (s <sup>-1</sup> )	$W_{xz}$ (s <sup>-1</sup> )	$W_{yz}$ (s <sup>-1</sup> )	$k_1$ (s <sup>-1</sup> ) <sup>c</sup>	$k_{av}$ (s <sup>-1</sup> ) <sup>d</sup>	$\Phi_f$ <sup>e</sup>	$\nu_{1/2}(D - E)^f$	$\nu_{1/2}(2E)^f$
Trp (air eq)/406.7	0.306 (1)	0.102(5)	0.000 (4)	0.013(4)	0.040(6)	0.044(1)	0.141	0.136	0.35	50(2)	103(1)
Trp (Ar purged)	0.300(5)	0.099(3)	0.000(2)	0.014(2)	0.030(3)	0.047(1)	0.131	0.133	0.38	—	—
Trp (O <sub>2</sub> satd.)	0.30(1)	0.102(4)	0.000(1)	0.041(3)	0.049(5)	0.045(1)	0.129	0.132	0.48	—	—
Trp (deuter. glass)	0.282(8)	0.090(4)	0.000(3)	0.017(3)	0.026(4)	0.039(1)	0.114	0.124	0.36	68(2)	128(3)
W220Y AP Trp <sup>109</sup> /414.5	0.39(2)	0.101(9)	0.003(7)	0.050(7)	0.03(1)	0.040(1)	0.160	0.166	0.33	7(2)	—
wt AP Trp <sup>109</sup> /414.5	0.40(1)	0.106(7)	0.004(5)	0.034(6)	0.030(8)	0.040(1)	0.154	0.170	0.30	7.0(5)	18(1)
wt AP Trp <sup>220</sup> /411.4	0.39(1)	0.113(4)	0.000(3)	0.005(3)	0.045(5)	0.040(1)	0.171	0.168	0.30	43(2)	94(1)
H74W LacRep Trp <sup>74</sup> /413	0.38(1)	0.113(4)	0.000(3)	0.008(3)	0.036(4)	0.039(1)	0.155	0.163	0.32	48(1)	91(5)
H74W + IPTG Trp <sup>74</sup> /419	0.40(1)	0.127(6)	0.004(4)	0.010(1)	0.031(6)	0.048(1)	0.168	0.177	0.44	42.2(3)	82(2)
Y273W LacRep Trp <sup>273</sup> /415	0.35(1)	0.114(5)	0.000(3)	0.033(4)	0.033(6)	0.065(1)	0.158	0.155	0.44	41(1)	73(3)
Y273W + IPTG Trp <sup>273</sup> /413	0.35(2)	0.096(5)	0.000(3)	0.034(7)	0.04(1)	0.091(1)	0.146	0.153	0.53	27(1)	58(3)
W201Y LacRep Trp <sup>220</sup> /410	0.323(7)	0.090(3)	0.004(2)	0.025(2)	0.031(4)	0.0498(4)	0.141	0.139	0.40	43(1)	97(2)
W201Y + IPTG Trp <sup>220</sup> /408.5	0.35(1)	0.096(5)	0.000(3)	0.020(4)	0.023(5)	0.0711(5)	0.143	0.149	0.32	38.7(3)	96(1)
holo W19,99Y TrpRep/410.2	0.33(2)	0.10(1)	0.000(3)	0.010(6)	0.068(9)	0.025(1)	0.131	0.143	0.45	35(3)	83(5)
RNase T1 Trp <sup>59</sup> /405.2	0.32(7)	0.09(4)	0.05(3)	0.00(3)	0.01(4)	0.063(6)	0.149	0.153	0.35	35(2)	54(1)
NCp7 Trp <sup>37</sup> /409.6	0.35(3)	0.09(1)	0.000(8)	0.00(1)	0.06(2)	0.05(3)	0.150	0.146	0.39	52(1)	122(2)
NCp7+poly I Trp <sup>37</sup> /415.8	0.49(2)	0.11(1)	0.00(1)	0.06(1)	0.05(1)	0.050(1)	0.199	0.200	0.44	70(2)	179(8)

<sup>a</sup> Standard errors ( $\sigma_e$ ) in last digit are given in brackets. <sup>b</sup>  $\lambda_{0,0}$  is the Trp 0,0-band peak in nm. <sup>c</sup> Decay constant of the population with rapid SLR, see text; estimated error is  $\pm 0.003$ . <sup>d</sup> Phosphorescence decay rate constant at 4.2 K; estimated error is  $\pm 0.003$ . <sup>e</sup> Estimated error  $< \pm 0.02$ . <sup>f</sup> ODMR bandwidth (half-width at half-maximum intensity), in MHz.

changes in phosphorescence wavelength, ODMR bandwidths (Table 1), and frequencies.<sup>29</sup> Ligand binding also produces changes in the efficiency of disorder mode SLR, represented by  $\Phi_f$ . For each mutant, IPTG binding leads to narrower ODMR bandwidths, but the  $\Phi_f$  in H74W LacRep and Y273W LacRep increases whereas it decreases in W201Y LacRep. In addition, the IPTG complex of Y273W LacRep that has the narrowest ODMR bands of the LacRep samples has the largest  $\Phi_f$  (0.53). It is interesting that H74W LacRep has relatively inefficient disorder mode-induced SLR ( $\Phi_f = 0.32$ ); although its Trp site is among the most inhomogeneous as determined by ODMR bandwidths. Clearly, there appears to be no relationship between the heterogeneity of the local Trp environment and the efficiency of disorder mode-induced SLR.

**Ribonuclease T1.** RNase T1 has been investigated previously in detail;<sup>20</sup>  $\Phi_f$  was found to vary with solvent composition in EG–buffer mixtures, displaying a broad minimum (0.35) near 40% EG by volume. The solvent dependence, which is similar to that of free Trp, could be related to the position of the Trp residue near the surface of the enzyme, hydrogen bonded to an internal water molecule.<sup>42</sup> We have not investigated the solvent dependence of SLR in any protein with a Trp buried in an internal hydrophobic fold, such as Trp<sup>109</sup> of AP. Among the proteins investigated in this work, the RTP of only AP and RNase T1 have been studied to our knowledge; the RTP lifetime of RNase T1, ca. 14 ms,<sup>26</sup> is considerably shorter than that of AP, suggesting that  $\Phi_f$  at 1.2 K might have an inverse relationship to site rigidity and RTP lifetime.

**Tryptophan Repressor Protein.** The binding of the Trp corepressor to tryptophan-free apo trpRep affects the triplet state properties of the corepressor. Changes in the ODMR frequencies, bandwidths, and kinetic parameters have been reported previously;<sup>32</sup> some of these data are given in Table 1. Trp binds to a hydrophobic cleft in apo trpRep leading to a red shift in the phosphorescence and a reduction in ODMR bandwidths (Table 1) consistent with a more homogeneous and polarizable environment relative to the aqueous EG glass. In analyzing the phosphorescence decay kinetics at 1.2 K, we find that  $\Phi_f$  of Trp increases from 0.35 to 0.45 when bound to the corepressor site of trpRep. Although the Trp binding site is more homogeneous than that in the solvent glass, relaxation via disorder modes is more efficient.

**Nucleocapsid Protein from HIV-1, NCp7.** This 55 amino acid peptide binds to single-stranded and double-stranded nucleic

acids.<sup>43</sup> Its main structural elements are two tandem zinc fingers, one of which incorporates a Trp residue. Aromatic stacking interactions affect the triplet state properties of the single Trp residue when NCp7 is bound to single-stranded nucleic acids, including polyinosinic acid (poly I).<sup>35</sup> Some relevant properties of NC p7 and its poly I complex are listed in Table 1. The large red shift, decay rate constant enhancement, and reduction of the zfs parameters<sup>35</sup> are attributed to stacking interactions with the hypoxanthine bases of poly I. Based on ODMR bandwidths, the heterogeneity of the Trp environment in NCp7 is comparable to free Trp in the same aqueous EG glass, but the value of  $\Phi_f$  is slightly larger, suggesting that disorder mode-induced SLR is somewhat more efficient. The ODMR bandwidths increase in the complex of NCp7 and poly I, indicating that the Trp environment in the complex is more heterogeneous than in free NCp7. In this case, the disorder mode activity increases, as well, in the poly I complex.

**Estimating  $W_f$  from  $k_1$  and  $k_{2(3)}$ .** Although the SLR model for the  $n_f^0$  population is simplified, it may be possible to obtain a rough estimate of the effective SLR rate constant,  $W_f$ , from the values of  $k_1$  and  $k_{2(3)}$  obtained from the decay analysis. In this model it is assumed that the  $k_i$  are the same for each population. From the analysis of H74W LacRep shown in Figure 3, we have fitted the initial transient shown in the residuals plot, E, to a single exponential using a nonlinear least-squares procedure, from which we obtain  $k_{2(3)} = 1.3 (\pm 0.1) \text{ s}^{-1}$ . From a calculation analogous to that plotted in Figure 2, but using the  $k_i$  of H74W LacRep given in Table 1, this value of  $k_{2(3)}$  corresponds to  $W_f = 0.38 \text{ s}^{-1}$  for this protein.  $W_f$  is small enough that  $k_1$  should be measurably less than  $k_{av}$  (Figure 2), and calculation gives  $k_1 = 0.143 \text{ s}^{-1}$ . This is less than  $k_{av}$  (0.163  $\text{s}^{-1}$ ), but it is also less than the measured value of  $k_1$  (0.155  $\text{s}^{-1}$ ); the measured value of  $k_1$  would require  $k_{2(3)} = 2.5 \text{ s}^{-1}$  and  $W_f = 0.8 \text{ s}^{-1}$ . These discrepancies likely are due to a combination of experimental uncertainties, particularly in  $k_{2(3)}$ , and the crudeness of the kinetic model used for  $n_f^0$ . A significant portion of the initial transient (2–3% of the total intensity) could be due to phosphorescence from impurities present in the EG that we have found impossible to eliminate completely. Thus  $k_1$  is probably a better indicator of the value of  $W_f$  in this model. It is possibly significant that the largest differences in  $k_{av}$  and  $k_1$  are found when  $k_{av} > k_1$ . In all, eleven samples have  $k_1 < k_{av}$ , the average difference being 0.008, while five have  $k_1 > k_{av}$ , and the average difference for these is 0.003. It appears

that for some of these samples,  $W_f$  may be as small as  $0.8\text{ s}^{-1}$ , but it may be considerably larger for others for which  $k_1 \approx k_{av}$ .

## Summary

SLR in the triplet state of Trp has been investigated in a number of protein sites at 1.2 K using ODMR in zero applied magnetic field. The matrix is aqueous EG glass. In each sample we find, as in earlier work, that the phosphorescence decay corresponds to a distribution of SLR rate constants, that is apparently bimodal. A population,  $n_s^0$ , is characterized by slow (crystal-like) SLR rate constants as determined from global analysis of MIDP data sets, while the remaining population,  $n_f^0$ , decays with rapid SLR rate constants (relative to the decay rate constant), and does not contribute to the ODMR signals. The latter population is coupled to disorder (tunneling) modes present in the matrix that produce efficient SLR by modulation of the EED interaction. These modes are not present in a crystalline matrix, and previous ODMR measurements<sup>10</sup> confirm the absence of  $n_f^0$  in such systems. Analysis of the phosphorescence decay yields  $\Phi_f$ , the fraction of the population undergoing rapid SLR.  $\Phi_f$  is found to vary considerably between samples, ranging from a low of 0.30 in AP, to a high of 0.53 in the IPTG complex of Y273W LacRep. We find no correlation between  $\Phi_f$  and the heterogeneity of the Trp site as determined by the ODMR bandwidths. In fact,  $\Phi_f$  of free Trp in aqueous EG glass is smaller than in a number of protein sites with narrower ODMR bandwidth. It is suggested that low disorder mode activity at cryogenic temperatures may be related to greater rigidity of the Trp environment, which at higher temperatures has been associated with long RTP lifetimes. The rigidity of a protein site may be retained at high temperature by an extended molecular structure, while the rigidity of an aqueous EG glass is lost as it softens. The RTP lifetimes of AP and RNase T1 have been measured, and bear an inverse relationship to  $\Phi_f$  in agreement with this suggestion.

We find no significant differences in the kinetics of Trp in air-equilibrated aqueous EG glass and in Ar-purged glass at 1.2 K, indicating no measurable influence of dissolved  $O_2$  on SLR in the air-equilibrated matrix. In  $O_2$ -saturated glass, however, a significant increase is found in  $\Phi_f$ . Deuteration of the solvent has no effect on  $\Phi_f$  but decreases  $k_{av}$  by 9%. This is likely to result mainly from deuterium exchange of the N–H proton of the indole ring.

The glassing solvent used in these studies, 30–40% EG–water (v/v), appears to provide a unique matrix for ODMR studies of triplet states. In unpublished MIDP measurements on indole we find SLR rate constants in this glass that are comparable to those of Trp, but they are larger by an order of magnitude in nonpolar glasses such as methylcyclohexane, 3-methylpentane, methyltetrahydrofuran, and perfluorohexane. ODMR signals are very weak in these solvents because of reduced spin alignment in the triplet state. This suggests that polar interactions make a significant contribution to the rigidity of the matrix at low temperature.

**Acknowledgment.** We are grateful to Professors Maurice Eftink, Ari Gafni, and Kathleen S. Matthews for many of the protein samples used in this work. This research was partially supported by Grant ES-02662 from the National Institute of Environmental Health Sciences, DHHS. The contents of this paper are solely the responsibility of the authors and do not necessarily reflect the views and policies of NIEHS, DHHS.

## References and Notes

- (1) Bowman, M. K.; Kevan, L. In *Time Domain Electron Spin Resonance*; Kevan, L., Schwartz, R. N., Eds.; Wiley: New York, 1979; p 67.
- (2) Abragam, A.; Bleaney, B. *Electron Paramagnetic Resonance of Transition Ions*; Clarendon: Oxford, U.K., 1970; Chapter 10.
- (3) Dalton, L. R.; Kwiram, A. L.; Cowen, J. A. *Chem. Phys. Lett.* **1972**, *14*, 77.
- (4) Dalton, L. R.; Kwiram, A. L.; Cowen, J. A. *Chem. Phys. Lett.* **1972**, *14*, 495.
- (5) Wolfe, J. P. *Chem. Phys. Lett.* **1971**, *10*, 212.
- (6) Konzelmann, U.; Kilpper, D.; Schwoerer, M. *Z. Naturforsch.* **1975**, *30A*, 754.
- (7) Anthunis, D. A.; Botter, B. J.; van der Waals, J. H. *Chem. Phys. Lett.* **1975**, *36*, 225.
- (8) Verbeek, P. J. F.; van't Hoff, C. A.; Schmidt, J. *Chem. Phys. Lett.* **1977**, *41*, 292.
- (9) Ghosh, S.; Petrin, M.; Maki, A. H. *J. Chem. Phys.* **1987**, *86*, 1789.
- (10) Ozarowski, A.; Wu, J. Q.; Maki, A. H. *Chem. Phys. Lett.* **1998**, *286*, 433.
- (11) van Vleck, J. H. *Phys. Rev.* **1940**, *57*, 426.
- (12) Bowman, M. K.; Kevan, L. *J. Phys. Chem.* **1977**, *81*, 456.
- (13) Brenner, H. C.; Kolubayev, V. *J. Luminescence* **1988**, *39*, 251.
- (14) Kaiser, G.; Friedrich, J. *J. Phys. Chem.* **1991**, *95*, 1053.
- (15) Kaiser, G.; Perron, H.; Friedrich, J. *J. Chem. Phys.* **1993**, *99*, 605.
- (16) Tringali, A.; Brenner, H. C. *Chem. Phys.* **1998**, *226*, 187.
- (17) Phillips, W. A. *J. Low Temp. Phys.* **1972**, *7*, 351.
- (18) Anderson, P. W.; Halperin, B. I.; Varma, C. M. *Philos. Mag.* **1972**, *25*, 1.
- (19) Phillips, W. A., Ed. *Amorphous Solids: Low-Temperature Properties*; Springer: Berlin, 1981.
- (20) Wu, J. Q.; Ozarowski, A.; Maki, A. H. *J. Phys. Chem. A* **1997**, *101*, 6177.
- (21) For reviews see, Kwiram, A. L.; In *Triplet State ODMR Spectroscopy. Techniques and Applications to Biophysical Systems*; Clarke, R. H., Ed; Wiley: New York, 1982; p 427. Maki, A. H. In *Biological Magnetic Resonance*; Berliner, L. J., Reuben, J., Eds.; Plenum: New York, 1984; Vol. 6, p 187. Hoff, A. J. *Methods Enzymol.* **1994**, *227*, 290.
- (22) McGlynn, S. P.; Azumi, T.; Kinoshita, M. *Molecular Spectroscopy of the Triplet State*; Prentice Hall: Englewood Cliffs, NJ, 1969.
- (23) Schmidt, J.; Veeman, W. S.; van der Waals, J. H. *Chem. Phys. Lett.* **1969**, *4*, 341.
- (24) Ozarowski, A.; Wu, J. Q.; Maki, A. H. *J. Magn. Reson. A* **1996**, *121*, 178.
- (25) Andreev, V. A.; Prilutskii, Yu. I. *Low Temp. Phys.* **1993**, *19*, 952.
- (26) Vanderkooi, J. M.; Calhoun, D. B.; Englander, S. W. *Science* **1987**, *236*, 568.
- (27) Strambini, G. B.; Gonnelli, M. *J. Am. Chem. Soc.* **1995**, *117*, 7646.
- (28) Gardner, J. A.; Matthews, K. S. *J. Biol. Chem.* **1990**, *265*, 21061.
- (29) Ozarowski, A.; Barry, J. K.; Matthews, K. S.; Maki, A. H. *Biochemistry* **1999**, *38*, 6715.
- (30) Barry, J. K.; Matthews, K. S. *Biochemistry* **1997**, *36*, 15632.
- (31) Mann, C. J.; Royer, C. A.; Matthews, C. R. *Protein Sci.* **1993**, *2*, 1853.
- (32) Ozarowski, A.; Wu, J. Q.; Maki, A. H. *FEBS Lett.* **1998**, *422*, 52.
- (33) Fischer, C. J.; Schauerte, J. A.; Wissner, K. C.; Gafni, A.; Steel, D. G. *Biochemistry* **2000**, *39*, 1455.
- (34) Ghosh, S.; Misra, A.; Ozarowski, A.; Stuart, C.; Maki, A. H. *Biochemistry* **2001**, *40*, 15024.
- (35) Wu, J. Q.; Ozarowski, A.; Maki, A. H.; Urbaneja, M. A.; Henderson, L. E.; Casas-Finet, J. R. *Biochemistry* **1997**, *41*, 112506.
- (36) Wu, J. Q.; Ozarowski, A.; Maki, A. H. *J. Magn. Reson. A* **1996**, *119*, 82.
- (37) Wu, J. Q.; Ozarowski, A.; Davis, S. K.; Maki, A. H. *J. Phys. Chem.* **1996**, *100*, 11496.
- (38) Martin, T. E.; Kalantar, A. H. In *Molecular Luminescence*; Lim, E. C., Ed.; Benjamin: New York, 1969; p 437.
- (39) Lin, S. H.; Bersohn, R. *J. Chem. Phys.* **1968**, *48*, 2732.
- (40) Hirota, N.; Hutchison, C. A., Jr. *J. Chem. Phys.* **1967**, *46*, 1561.
- (41) Schauerte, J. A.; Steel, D. G.; Gafni, A. *Methods Enzymol.* **1997**, *278*, 49.
- (42) Arni, R.; Heinemann, U.; Tokuoka, R.; Saenger, W. *J. Biol. Chem.* **1988**, *263*, 15383.
- (43) Maki, A. H.; Ozarowski, A.; Misra, A.; Urbaneja, M. A.; Casas-Finet, J. R. *Biochemistry* **2001**, *40*, 1403.